

THEORETICAL CRITICAL HEAT FLUX PREDICTION BASED ON NON-EQUILIBRIUM THERMODYNAMICS CONSIDERATIONS OF THE SUBCOOLED BOILING PHENOMENON

Germán Theler^a and Daniel Freis^b

^a*TECNA Estudios y Proyectos de Ingeniería S.A.
Encarnación Ezcurra 365, C1107CLA Buenos Aires, Argentina*

^b*Westinghouse Electric Germany GmbH
Dudenstraße 44, 68167 Mannheim, Germany*

Keywords: Critical Heat Flux, Departure of Nucleate Boiling, Subcooled Boiling

Abstract. Whenever power is to be transferred from a heated surface to a liquid coolant, it is usually desired to obtain high heat fluxes with low temperature differences to avoid excessive stress in mechanical components. For single-phase forced flows, there is a linear relationship between the heat flux and the temperature difference. If the heat flux is increased, some bubbles nucleate at the hot surface and then they depart to the subcooled fluid bulk where they collapse. This subcooled boiling regime enhances transference and tends to give higher heat fluxes for the same temperature difference than in pure single-phase convection. However, if the heat flux is further increased, at some point a vapor film is formed on the hot surface. The heat transfer rate is suddenly reduced and the wall temperature increases, usually up to prohibitive values. This dry-out phenomenon is known as departure of nucleate boiling (DNB), and the value of the heat flux at which it occurs is called the critical heat flux (CHF). As this value poses an upper bound to the rate at which heat can be extracted from a certain source, its prediction is of central importance in the design of heat removal systems. In this paper a theoretical derivation of the DNB wall temperature for low void fraction is proposed based on non-equilibrium thermodynamics considerations of the subcooled boiling phenomenon. Then, using two-phase heat-transfer correlations, values for the actual CHF are estimated. These predictions are applied and compared to empirical observations in a mathematical model of a nuclear reactor channel, as this subject is of special concern in the nuclear industry because although virtually an infinite power can be generated by fission of the uranium in the fuel, the actual thermal power is limited by the efficiency of the core cooling systems.

1 INTRODUCTION

The critical heat flux poses a limit for the efficient heat removal of industrial systems of interest. It is very important to be able to estimate its value from the engineering point of view mainly for two reasons. A good heat removal system should work as near as possible to the critical heat flux to obtain high heat fluxes involving only moderately low temperature differences. Thus, a correct estimation of this value is desired in order to define the design point of the system. On the other hand, when performing transient deterministic safety analysis for postulated accidents where the critical heat flux is expected to be passed, its value is important to correctly select the appropriate models according to the heat transfer regime.

There is not yet a sound theory able to explain how two-phase heat transfer works for every combination of flow pattern and energy transfer condition, and thus the critical heat flux is usually estimated using empirical correlations. Moreover, not only the general geometry but also other particular obstacles influencing flow development do affect also the critical heat flux. So, in general there are a number of correction factors that should be applied to the correlations making the problem highly sensitive to input data and rendering the results very inaccurate.

This concern about critical heat flux is of particular importance in both the design and the analysis of nuclear reactor cores, as in this case virtually an infinite amount of power can be generated in the fuel due to fission of uranium nuclei. The actual thermal power is given by the heat removal capacity of the coolant system, usually comprised of a forced flow of pressurized water. Deterministic safety analysis computer codes usually rely on a series of experimental correlations that are further corrected according to the geometry and the local patterns.

A method for estimating the wall temperature at which departure of nucleate boiling occurs based on theoretical considerations only without involving any experimental coefficient was first suggested by the authors (Freis et al., 2011). A new theory for the process of subcooled nucleate boiling introduced by Schroeder-Richter and Bartsch (1994) and one-dimensional momentum conservation equations are used to obtain a sonic limit for the heat transferred from a heated wall to a bulk fluid involving the generation of bubbles. Afterwards, using then Chen (1963) correlation for subcooled boiling heat transfer, the actual value of the critical heat flux is estimated. Results are presented, compared to other methods and further discussed.

2 SUBCOOLED BOILING

Consider a solid body—that for the sake of simplicity will be considered as a plane heated wall—generating a certain thermal power that is to be removed by a convective flow of a fluid in contact with the wall. If the wall temperature T_w is lower than the saturation temperature T_s of the fluid, it will remain in single-phase conditions at all points of space. However, if T_w is greater than T_s , some boiling will occur even though the conditions far away from the wall are such that the bulk fluid is still subcooled. This situation is called subcooled boiling, and is usually desired to reach it in heat removal systems design. This is important because of two reasons: the bulk fluid is liquid and thus stable and easy to handle and bubble generation improve heat transfer rates.

For highly subcooled bulk flow, bubbles generated at the wall surface collapse before moving a great distance and they produce no net effect. In this case, they do not significantly change neither hydrodynamic nor heat transfer conditions. This situation is known as wall void (figure 1). However, for higher bulk temperatures, depending on flow patterns and conditions, bubbles generated at the wall surface may move into the subcooled bulk fluid and then collapse. This detachment can be mainly due to thermal effects (for low Peclet numbers) or due to hydro-

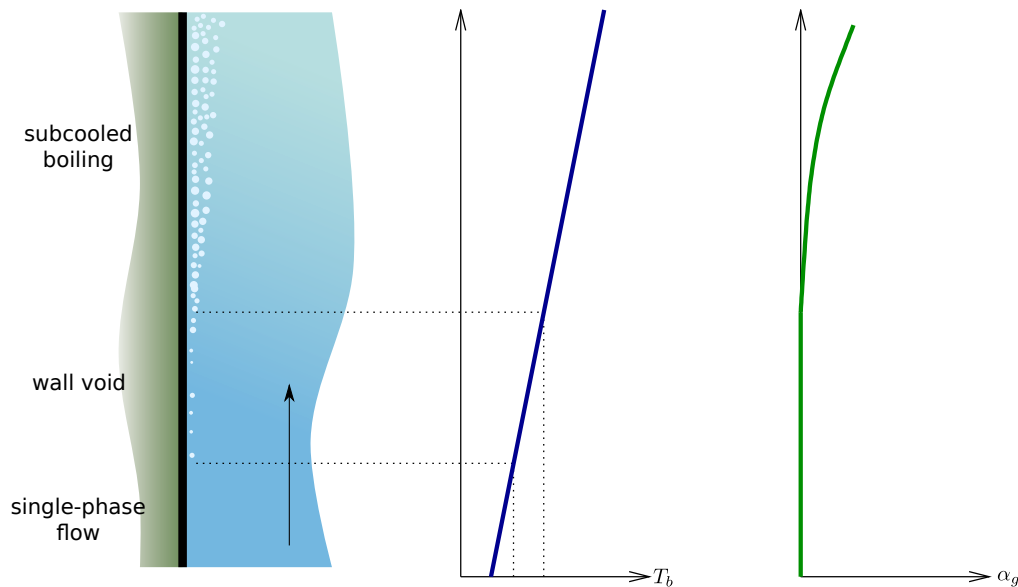


Figure 1: Uniformly heated planar wall in contact with a forced vertical flow. After single-phase flow, some bubbles are generated in wall void conditions but they collapse without detaching. After a certain point, nucleate boiling occurs. Bulk fluid temperature T_b increases linearly with the axial coordinate and void fraction is non-negligible in subcooled nucleate boiling conditions. Figure reproduced from [Theler \(2008\)](#).

dynamic effects (for high Peclet numbers) as discussed by [Clausse and Lahey \(1990\)](#). In any case, bubbles carry away heat and momentum and the heat transfer rate is greatly improved. Besides, some changes in the hydraulic conditions due to a higher head loss are also usually observed. These conditions are known as subcooled boiling (figure 1).

2.1 Boiling crisis and critical heat flux

Almost eighty years ago, [Nukiyama](#) performed a series of experiments to investigate how heat is transferred from a solid to a fluid under subcooled boiling conditions. By controlling the total power generated, he measured the correlation between the heat flux and the wall temperature. The plot shown in figure 2 is widely known as the Nukiyama curve. For wall temperatures T_w slightly above the saturation temperature T_s of the fluid, no appreciable bubble generation is observed and the heat transfer increases linearly with the temperature difference. If the heat flux is increased (following the thick curve in figure 2), there exists a temperature T_{ONB} after which bubbles start to nucleate and the heat transfer is improved. The classical theory that explains what the mechanisms of bubble generation are, is briefly covered in section 2.2. However, a novel theory based on both thermodynamical and mechanical non-equilibrium, on which the present work is based, is introduced in section 2.3. In any case, the region of nucleate boiling is very convenient from the engineering point of view of heat removal systems as it provides high heat transfer rates with moderately low temperature differences.

According Nukiyama's results, the heat flux and the wall temperatures present an hysteresis effect that poses a technological problem on heat transfer problems. There exists a certain point, known as departure of nucleate boiling, after which an infinitesimal increment in the heat flux produces a finite and extremely big increment in the wall temperature. In figure 2, T_w increases from T_{DNB} for \dot{q}''_{crit} to T_f for $\dot{q}''_{crit} + d\dot{q}''$ following the thick curve. Noting the logarithmic scale

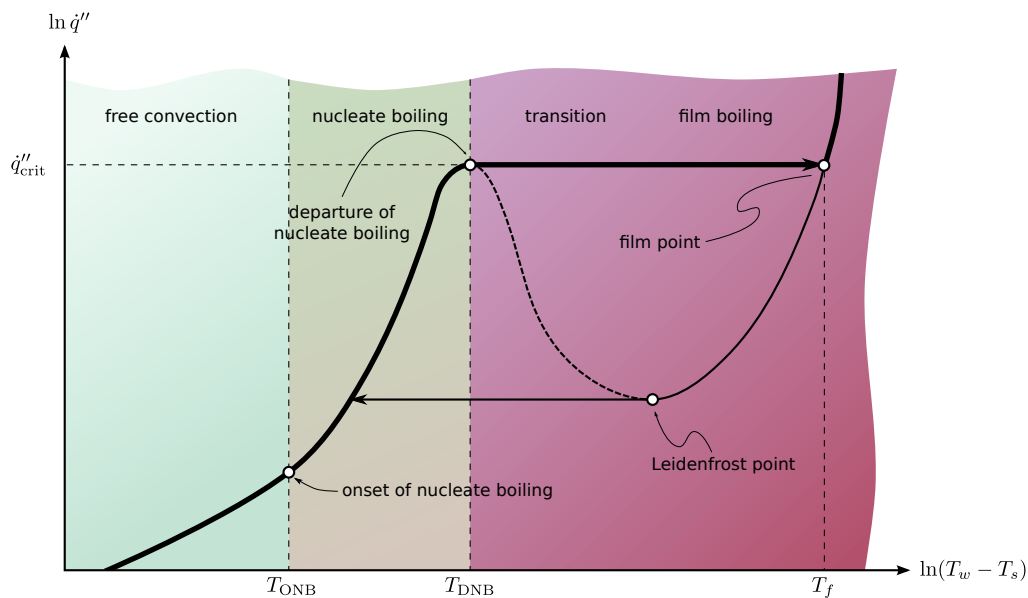


Figure 2: The Nukiyama curve and the subcooled boiling regimes

of the abscissas, T_f may be very much bigger than T_{DNB} , possibly comprising the structural integrity of the solid materials that compose the heated solid.

This is explained by noting that for high heat fluxes, bubbles do not form individually but a film of vapor is generated all over the heated surface. Thus, the heat transfer coefficient is highly reduced because the interphase is now solid-vapor instead of solid-liquid. Therefore, to transfer the same amount of heat as the previous case, the temperature difference has to increase significantly. Figure 3a shows experimentally a case of nucleate boiling and figure 3b shows what happens when the film point is reached. This sharp increment of the wall temperature is known as boiling crisis.

The hysteresis effect can be seen when decreasing the heat flux. In this case, the heat flux follows the path from the film point along the narrow line of the Nukiyama curve in figure 2 down to a temperature called the Leidenfrost point (Walker, 1977). If the power is further decreased, the wall temperature moves to the left through the straight narrow line back to the nucleate boiling regime. The dashed part of the Nukiyama curve in figure 2 can only be seen by controlling the wall temperature instead of the heat flux in the experiments.

By using dimensional analysis and experimental background, it is accepted that for a certain fluid in a fixed geometric configuration, the critical heat flux depends on the pressure, the local quality and the mass flux, i.e.

$$\dot{q}''_{\text{crit}} = f(p, x, G) \quad (1)$$

2.2 Classical nucleate boiling theory

In order to stress the differences with respect to the new theory the critical heat flux prediction this paper is based on, a brief review of the basic ideas of the classical theory on nucleate boiling is presented. The details and the actual equations are not very important. The main point is that this theory relies on a mechanical equilibrium that is maintained for every time of the bubble generation process.

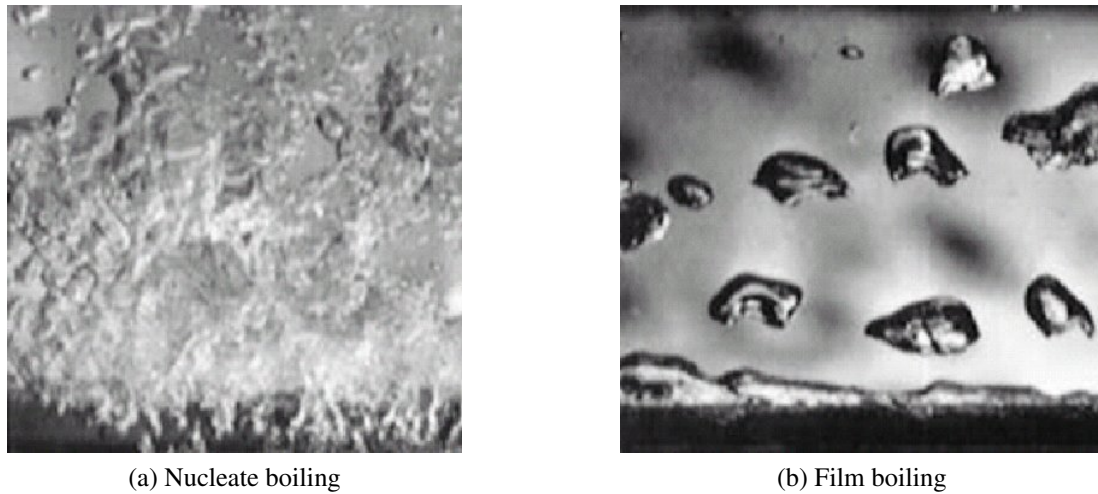


Figure 3: Photographs of heat transfer experiments for nucleate (left) and film (right) boiling. In case (a) bubble generation and detachment provides a very efficient mean to transfer heat with a moderately low temperature difference between the heated surface and the bulk fluid. In case (b) a film of vapor is created all over the heated surface and a great temperature difference is needed to remove the power generated. Pictures reproduced from [Clause \(2009\)](#).

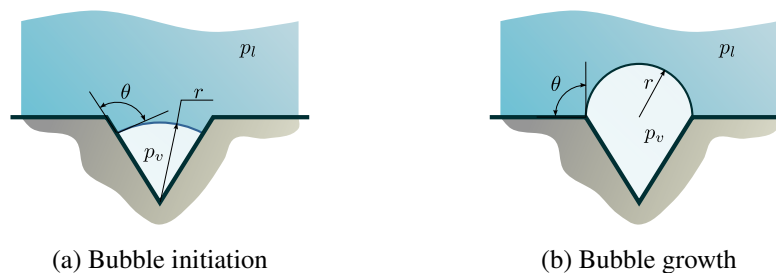


Figure 4: Bubble initiation and growth as explained by the classical nucleate boiling theory

The general approach used to explain nucleate boiling in the literature is based on the assumption of the existence of a superheated wall layer in metastable state. Whenever this state is disturbed, a new bubble is formed. This happens preferentially where a smooth heated surface contains pores, voids or roughness (figure 4a). The theory postulates that the formation of a bubble is initiated when a certain superheat is reached inside a pore and the metastable state is disturbed. The necessary vapor pressure inside the forming bubble is dependent of the radius and can be derived by a balance of forces in the early phase as

$$p_g - p_f = \frac{2\sigma}{r} \quad (2)$$

where p_g and p_f are the pressure in the vapor and liquid respectively, and σ is the surface tension between at the interphase. The Clausius-Clapeyron equation

$$\ln p = -\frac{h_{fg}M}{R} \frac{1}{T} + C \quad (3)$$

can be used to compute the temperature of the superheated vapor which is necessary to initiate bubble formation. In equation (3), p is pressure, h_{fg} is the enthalpy of evaporation, M is the molar mass, R is the ideal gas constant, T is the absolute temperature and C is an arbitrary constant.

Using the ideal gas state equation and equation (2), this results in

$$T_g - T_s = T_s \cdot \frac{2\sigma}{r} \cdot \frac{(v_g - v_f)}{h_{fg}}$$

The further development of the bubble is characterized by dynamic growth. The volume increases and the radius decreases (see figure 4b). The necessary pressure inside the bubble reaches its maximum when the minimum radius occurs at an angle $\phi = \pi/4$. The growing bubble obtains energy from the superheated wall layer. However, mechanical equilibrium is always maintained.

As stated at the beginning of the section, the details of the actual bubble initiation and growth are not important for the scope of the present work. The important point to note is that a mechanical equilibrium between phases is maintained for every time.

2.3 Mechanical non-equilibrium boiling theory

Schroeder-Richter and Bartsch (1994) derived a theory to explain nucleate boiling which can be used to predict the wall temperature at which departure from nucleate boiling occurs in a low-void two-phase flow. Although the approach is completely based on theoretical considerations—as thoroughly explained in Schroeder-Richter (1991)'s PhD thesis—it is based on two experimental observations made under subcooled boiling conditions:

1. vapor bubbles move with considerable radial velocity from the heated wall into the subcooled liquid
2. the whole surface of the heated wall is wet during nucleate boiling. A liquid microfilm is located even under the base of each bubble

From the first observation, Schroeder-Richter and Bartsch (1994) infer that the radial velocity is induced by a pressure p_w at the heated surface that is higher than the bulk pressure p_b . The second observation, i.e. the presence of a liquid microfilm, was reported by other authors as well (Moore and Mesler, 1961; Dwyer and Hsu, 1975; Mitrovic, 1985). To explain this observation, Schroeder-Richter and Bartsch assume that there exists no metastable state at all and thus non-equilibrium thermodynamics have to be applied. On the one hand, they postulate a mechanical non-equilibrium condition in the sense of $p_w > p_b$. And on the other hand, they state that a stable microfilm is possible if and only if the surface temperature T_w is smaller or equal than the saturation temperature at p_w . If a lower pressure was assumed, a gaseous or metastable state should have been seen.

The formation of a bubble is explained by pressure fluctuation in the saturated liquid. A nucleus is formed when such a fluctuation leads to a local pressure below the saturation pressure. The nucleus is not formed at the wall but in the laminar wall boundary layer. After a nucleus is formed, the first bubble growth is initiated by inertia forces. A microscopic liquid film is formed under the bubble. Conservation of momentum between the liquid phase in the microfilm and the gaseous phase in the bubble enables a pressure difference to be established.

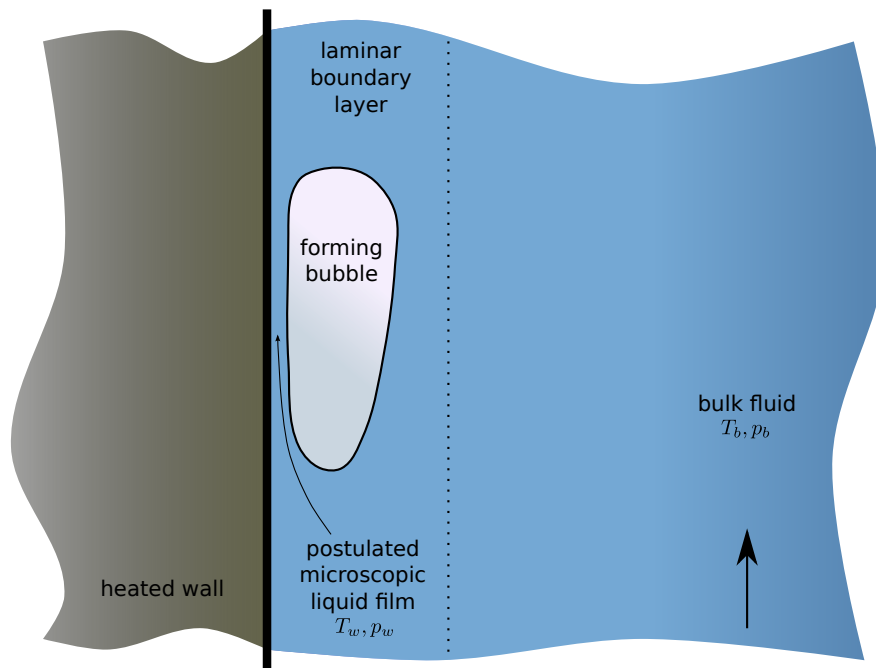


Figure 5: Forming bubble at a planar vertical heated wall and postulated liquid microfilm

According to [Schroeder-Richter and Bartsch](#), the pressure under the forming bubble can be estimated by using the Clausius-Clapeyron equation (3). By using the ideal gas equation of state and subtracting bulk from wall conditions

$$\ln p_w - \ln p_b = \frac{h_{fg}M}{R} \left[\frac{1}{T_s(p_b)} - \frac{1}{T_w} \right]$$

where p_w and p_b are the wall and bulk pressures respectively, $T_s(p_b)$ is the saturation temperature at bulk pressure and T_w is the wall temperature.

2.4 Departure of nucleate boiling

The evaporating mass flow is transported from the heated microfilm into the forming bubble, and the accelerating molecules preserve the pressure inside the film. This effect can be explained by a balance of momentum around the microfilm. [Schroeder-Richter and Bartsch](#) developed a one-dimensional model—along the direction perpendicular to the wall surface—that predicts a maximum boiling heat flux whenever either the bubble surface facing the bulk fluid moves away from the wall at the speed of sound in the liquid phase or the bubble surface facing to the wall moves at the speed of sound in the vapor phase with respect to the fixed wall. As the model applies to single bubbles, this maximum heat flux is the critical heat flux at which departure of nucleate boiling occurs. The other possible maximum heat flux is the dry-out, that is not covered by the low-void assumption.

The two aforementioned sonic conditions can be written as implicit equations on the temperature at which departure of nucleate boiling occurs

$$\left[v_g(p_b) - v_f(p_s(T_{\text{DNB}})) \right] \cdot \left[p_s(T_{\text{DNB}}) - p_b \right] = 2 a_g^2(p_b) \quad \text{if } 2a_g(p_b) < a_f(p_s(T_{\text{DNB}})) \quad (4)$$

$$\left[v_g(p_b) - v_f(p_s(T_{\text{DNB}})) \right] \cdot \left[p_s(T_{\text{DNB}}) - p_b \right] = \frac{1}{2} a_f^2(p_s(T_{\text{DNB}})) \quad \text{if } 2a_g(p_b) > a_f(p_s(T_{\text{DNB}})) \quad (5)$$

with T_{DNB} being the wall temperature at which departure of nucleate boiling occurs, T_s the saturation temperature at the bulk pressure, v_g and v_f the vapor and liquid specific volumes respectively, p_s the saturation pressure and a_g the speed of sound in the vapor phase and a_g in the liquid.

The temperature T_{DNB} can be computed from the implicit equations (4) and (5) using an appropriate equation of state for the substance and a suitable numerical scheme. For low pressures (less than 1.5 MPa for water), the second condition is the usual limit. An explicit expression for T_{DNB} can be obtained by using the speed of sound in the ideal gas, the ideal gas equation of state and the Clausius-Clapeyron equation (3). The result is

$$T_{\text{DNB}} = \frac{T_s(p_b)}{1 - \frac{R \cdot T_s(p_b)}{M \cdot h_{fg}(p_b)} \cdot \ln(2\kappa_g + 1)} \quad (6)$$

being κ_g the isentropic expansion factor that for ideal gases is

$$\kappa_g = -\frac{v}{p} \left(\frac{\partial p}{\partial v} \right)_s \approx \begin{cases} 1 + 2/3 & \text{for monatomic gases} \\ 1 + 2/5 & \text{for diatomic gases} \\ 1 + 1/3 & \text{for three-atomic gases} \\ \vdots & \end{cases}$$

The momentum conservation equations from which the sonic limit is obtained were derived for a one-dimensional case, i.e. applicable to an infinite plane heated wall. Nevertheless, for a definite coolant, the temperature T_{DNB} depends only on the bulk pressure p_b as can be seen in equations (4), (5) and (6). Figure 6—reproduced from [Schroeder-Richter and Bartsch \(1994\)](#)—shows a comparison of the predictions given by both the implicit and explicit equations with experimental results for different materials. A remarkable agreement between the theory and the experiment can be observed. On the one hand, this coincidence may suggest that the non-equilibrium theory may have some physical background and, on the other hand, that equations (4) and (5)—and eventually equation (6)—may be used to predict departure of nucleate boiling at the conditions they apply.

2.5 Critical heat flux

The fact that equation (6) agrees very well with experiments is a remarkable result, as the model it is based on relies only on non-equilibrium thermodynamics and momentum conservation. No empirical factor was introduced whatsoever. Nevertheless, to estimate the actual value of the critical heat flux \dot{q}''_{crit} from T_{DNB} , a heat transfer coefficient correlation is needed.

One of the most widely subcooled-boiling heat transfer correlations is that proposed by [Chen \(1963\)](#). In fact, this correlation is discussed in the paper by [Schroeder-Richter and Bartsch](#)

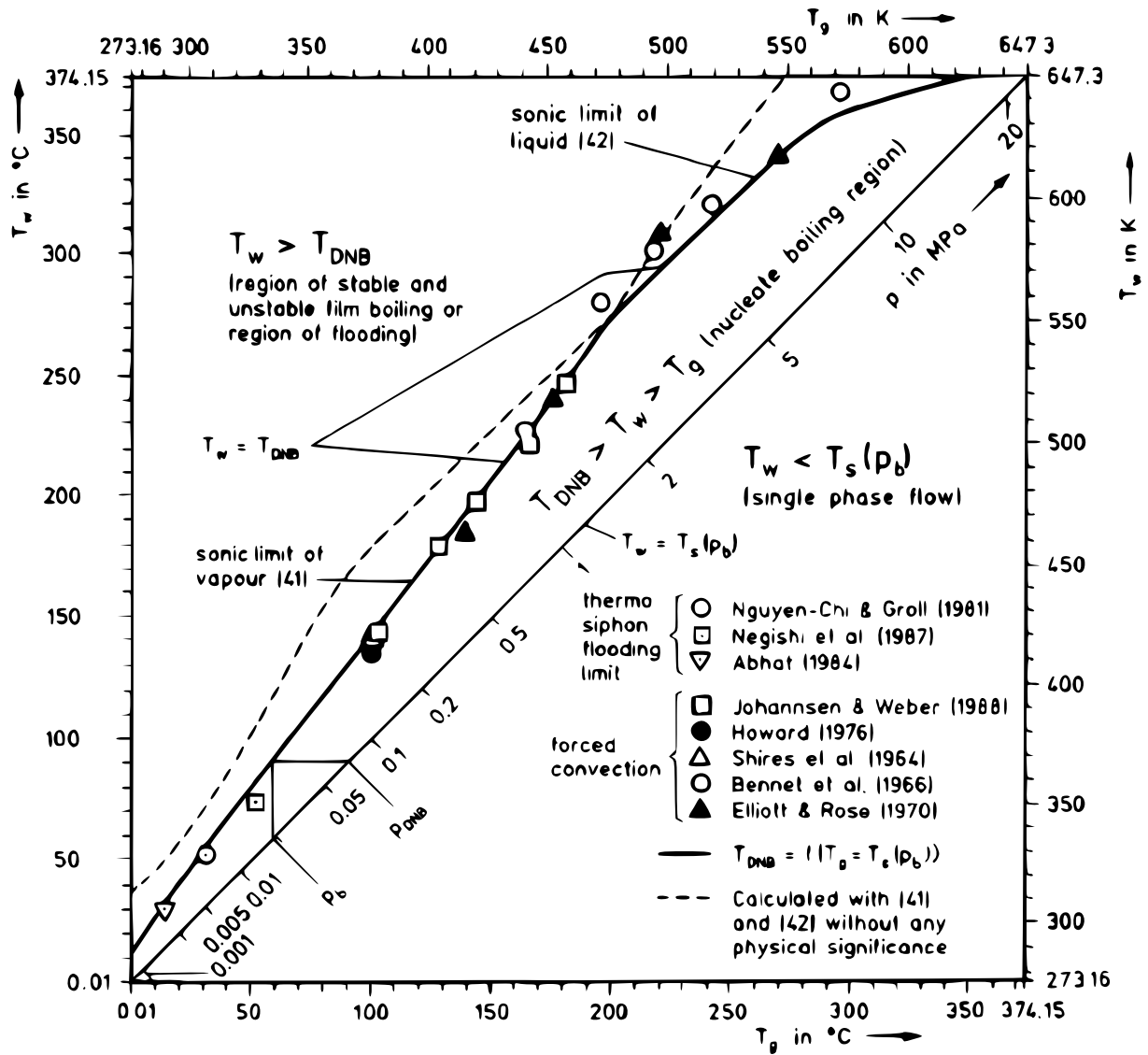


Figure 6: Comparison between experimental temperatures of departure of nucleate boiling with theoretical results obtained by using the mechanical non-equilibrium theory. Figure reproduced from Schroeder-Richter and Bartsch (1994). Equations labeled [41] and [42] in the figure are equations (4) and (5) in the present paper, respectively.

where they confirm the proposed dependence on the non-dimensional parameters under the light of the thermodynamical non-equilibrium theory they postulate. **Chen**'s correlation is separated into effects purely due to convection and effects of the boiling regime:

$$\dot{q}'' = \alpha_c \cdot (T_w - T_b) + \alpha_b \cdot (T_w - T_s) \quad (7)$$

The convective heat transfer coefficient α_c is calculated using the conventional Dittus-Boelter correlation plus a correction factor for positive qualities

$$\alpha_c = 0.023 \cdot \text{Re}^{4/5} \text{Pr}^{2/5} \cdot F(\chi_{tt}^{-1}) \cdot \frac{k_f}{D_H}$$

with Re and Pr the Reynolds and Prandtl numbers, k the thermal conductivity and D_H the hydraulic diameter. The Reynolds number factor $F(\chi_{tt}^{-1})$ is a function of the reciprocal Martinelli parameter

$$\chi_{tt}^{-1} = \begin{cases} 0 & \text{if } x \leq 0 \\ \left(\frac{x}{1-x}\right)^{0.9} \left(\frac{\rho_f}{\rho_g}\right)^{0.5} \left(\frac{\mu_g}{\mu_f}\right)^{0.1} & \text{if } x > 0 \end{cases}$$

where x is the quality, ρ is the density and μ is the static viscosity. The dependence of the Reynolds number correction factor with the reciprocal Martinelli parameter is approximated as

$$F(\chi_{tt}^{-1}) = \begin{cases} 1 & \text{if } \chi_{tt}^{-1} \leq 0.1 \\ 2.35 (\chi_{tt}^{-1} + 0.213)^{0.736} & \text{if } \chi_{tt}^{-1} > 0.1 \end{cases} \quad (8)$$

The boiling heat transfer coefficient, in watts per squared meter per Kelvin, is

$$\alpha_b \left[\frac{\text{W}}{\text{m}^2 \cdot \text{K}} \right] = 0.00068935 \cdot \left(\frac{k_f^{0.79} c_f^{0.45} \rho_f^{0.49} g^{0.25}}{\sigma_f^{0.5} \mu_f^{0.29} h_{fg}^{0.24} \rho_g^{0.24}} \right) (T_w - T_s)^{0.24} (p_s - p_b)^{0.75} \cdot S$$

with the new introduced quantities being c the constant-pressure heat capacity, g the gravity acceleration and μ the dynamic viscosity. For the equality to hold, all the units have to be in SI. Factor S is called the suppression factor and is defined as an effective superheat divided by the total superheat of the wall. It depends on a modified Reynolds number defined as¹

$$\text{Re}_{\text{TP}} = \text{Re} \cdot (1 - \alpha) \cdot [F(\chi_{tt}^{-1})]^{1.25}$$

approximately as (figure 7)

$$S(\text{Re}_{\text{TP}}) = \begin{cases} \frac{1}{1 + 3.305 \times 10^{-6} \cdot (\text{Re}_{\text{TP}})^{1.14}} & \text{Re}_{\text{TP}} < 325000 \\ \frac{1}{1 + 3.186 \times 10^{-4} \cdot (\text{Re}_{\text{TP}})^{0.78}} & 325000 \leq \text{Re}_{\text{TP}} \leq 700000 \\ 0.0797 & \text{Re}_{\text{TP}} > 700000 \end{cases} \quad (9)$$

¹In the literature there may appear a multiplicative factor 10^{-4} in the definition of Re_{TP} . However, in this paper this factor is incorporated in the dependence of the suppression factor $S(\text{Re}_{\text{TP}})$.

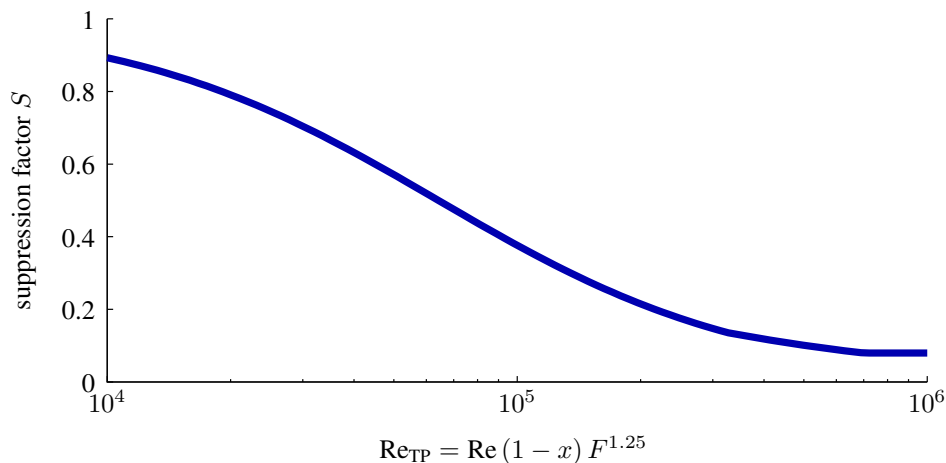


Figure 7: Suppression factor S vs. Re_{TP} as given by equation (9)

For high mass fluxes G , no-slip flow may be assumed and thus the void fraction α can be computed from the quality x by

$$\alpha = \frac{\frac{x}{\rho_g}}{\frac{(1-x)}{\rho_f} + \frac{x}{\rho_g}}$$

The critical heat flux is estimated by setting $T_w = T_{\text{DNB}}$ as predicted by the method proposed by [Schroeder-Richter and Bartsch](#) introduced in section 2.4. Summing up all the dependencies of every single function defined in these two sections, for a certain fluid the overall critical heat flux \dot{q}''_{crit} has the functional form

$$\dot{q}''_{\text{crit}} = f(p, x, G, D_H) \quad (10)$$

Comparing equation (10) to equation (1), it can be seen that the proposed method includes the geometric configuration as a single parameter, namely the hydraulic diameter. It should be stressed that the fact that the departure of nucleate boiling temperature was derived using a novel theory followed under a one-dimensional momentum conservation condition renders the computation of the critical heat flux using the proposed method just an approximate estimation for geometries of practical interest.

3 RESULTS

By using the estimation of the critical heat flux developed in the previous section, some results are shown in this one. First, a comparison of the two sonic limits given by equations (4) and (5) is performed. Then, a continuous four-dimensional function is computed and surface contours plots for different mass fluxes are shown. Some scattered points given by other CHF-estimation correlations are plotted in some of the figures. Finally, the method is applied to a very simplified nuclear reactor model in which a thermalhydraulic code is coupled to a neutronic code to obtain a steady-state power distribution. The code estimates a critical heat flux for the nucleate boiling region, that is compared to the estimation proposed in this work.

All the examples below use light water as the working fluid mainly because there is far more data on experimental critical heat flux measurements on water than on any other material. As

this method is under development and improvement, constant comparison is desired. However, one of its main advantages is that—at least for the temperature of departure—it does not rely on a single experiment coefficient that may depend on the substance. Thus, the method is expected to work with the same accuracy for light water, heavy water or benzene by just using the appropriate property tables.

The evaluation of the critical heat flux \dot{q}''_{crit} as proposed in section 2.5 requires the evaluation of explicit and implicit functions along with the interpolation of one and two-dimensional numerical data. This task can be implemented either in a high-level language such as Octave or directly at the calculation code in C or in Fortran. In particular, the results shown in the following three sections were obtained by employing the *wasora* framework. See appendix A for the actual input file used to implement the critical heat flux computation.

3.1 Temperature of DNB

As previously stated, the wall temperature at which departure of nucleate boiling is expected to occur according to equations (4) and (5)—or the explicit expression given by equation (6)—depends only on the bulk pressure p_b . Figure 8 shows the temperature of DNB as predicted by equations (4) and (5) along with the two conditions on the speed of sound as a continuous line. Note that the resulting T_{DNB} is actually the smaller temperature given by the two equations, although the actual temperature was computed from the conditions on the speed of sound. For low pressures, equation (4) applies whereas for high pressure (5) does.

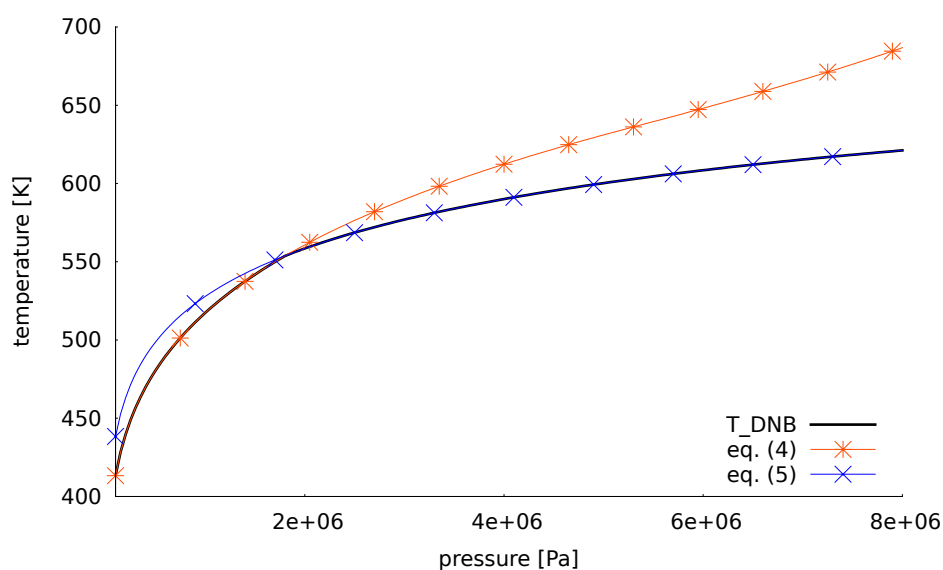
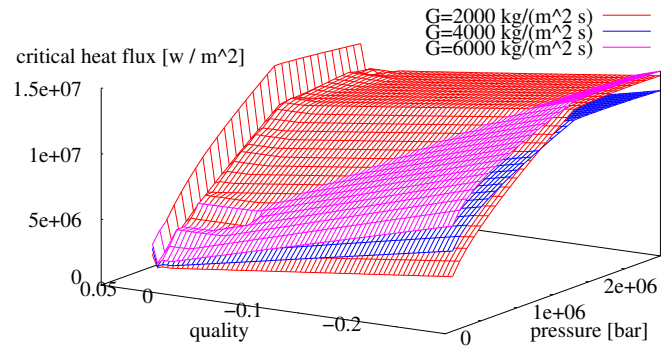


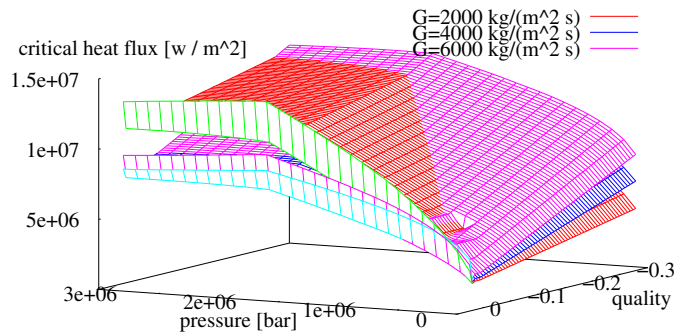
Figure 8: Wall temperature at which departure of nucleate boiling is expected to occur for water. Both sonic limits are shown, but the one given by the conditions on the speed of sound is taken as the actual DNB temperature.

3.2 Continuous CHF function

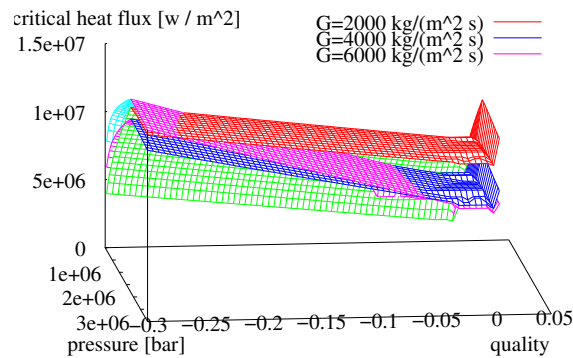
By using Chen's correlation, starting from the temperature of DNB, a function for the critical heat flux was developed. The resulting equation (7) is a function of the bulk pressure, the static quality, the mass flux and the hydraulic diameter, namely



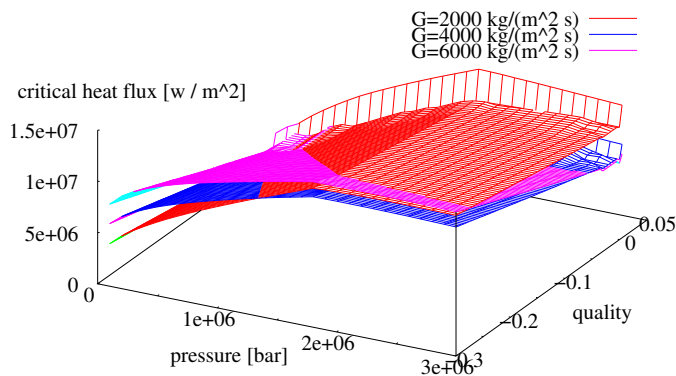
(a)



(b)



(c)



(d)

Figure 9: Surface contour plots of $q''_{crit}(p, x, G, D_H)$ for fixed $D_H = 8 \times 10^{-3}$ m and three different values of G .

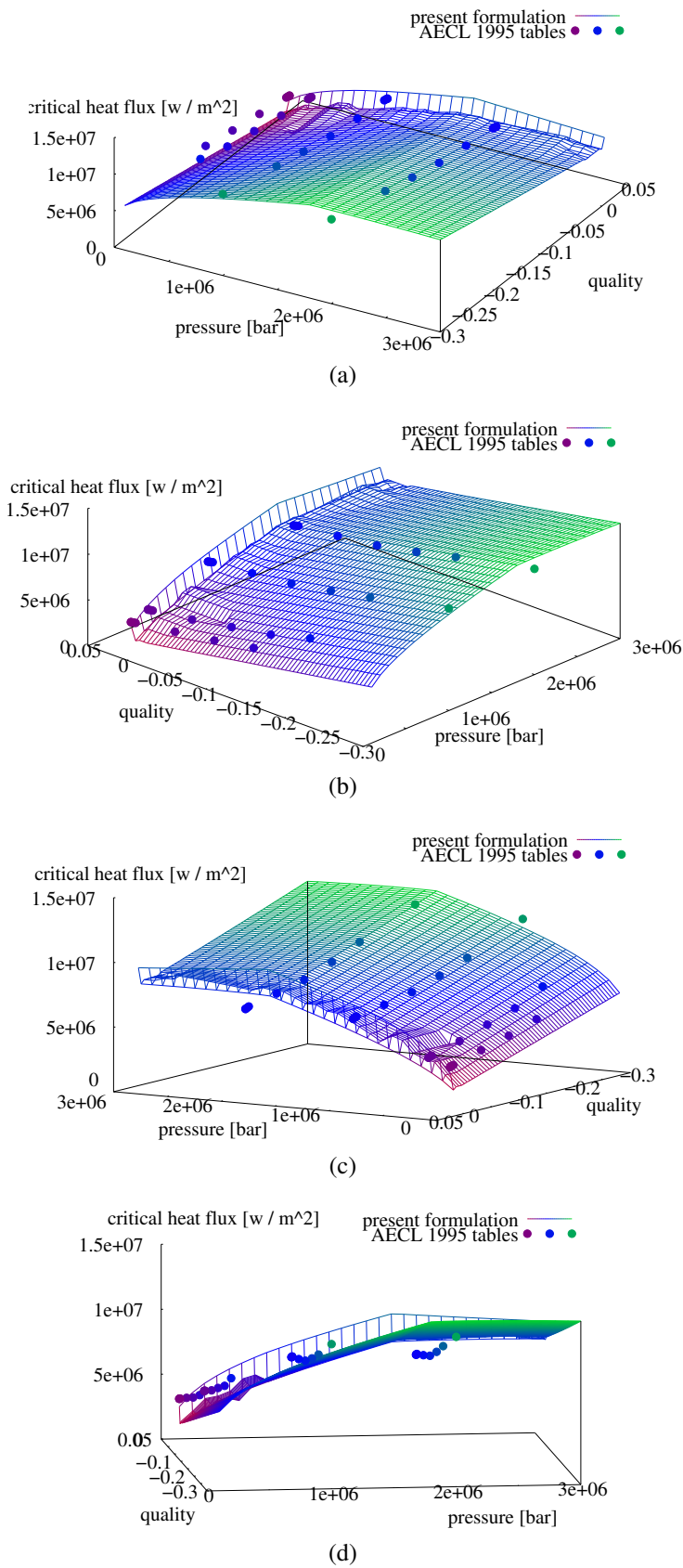


Figure 10: Comparison with the AECL 1955 look-up table (Groeneveld et al., 1996).

$$\dot{q}_{\text{crit}}'' = f(p, x, G, D_H)$$

Appendix A shows one way of computing this continuous function using the [wasora](#) framework. Of course, the presentation of a four-dimensional scalar field poses certain inconveniences, especially for plain-paper documents. Figures 9a–9d show four views of a surface contour plot fixing the hydraulic diameter to $D_H = 0.008$ m and for three values of the mass flux $G = 2000, 4000$ and 6000 $\text{kg} \cdot \text{m}^{-2} \cdot \text{s}^{-1}$.

Figures 10a–10d illustrate how the proposed method compares to the AECL 1995 CHF look-up tables ([Groeneveld et al., 1996](#)). The hydraulic diameter is fixed again to $D_H = 0.008$ m and the mass flux is set to $G = 4000$ $\text{kg} \cdot \text{m}^{-2} \cdot \text{s}^{-1}$. The color of the scattered points should be compared to the color of the continuous function $\dot{q}_{\text{crit}}'' = f(p, x, G, D_H)$. The discussion of the results is deferred to section 4.

3.3 Nuclear reactor channel model

Finally, an illustration of how this method compares to actual simulation computer codes estimations of the critical heat flux is given. A one-dimensional thermalhydraulic model implemented using RELAP—actually a modified version extended to be able to couple to other codes using shared memory objects ([Mazzantini et al., 2011](#))—was coupled to a one-dimensional nuclear reactor core model computed using the free neutronic diffusion code [milonga](#). Therefore, a non-trivial power profile—giving rise to non-trivial fuel and coolant temperature profiles—was obtained. The hydraulic conditions were selected such that nucleate boiling conditions were observed. Figure 11 shows the power profile and the two limits estimated by using RELAP's internal method of CHF estimation based on corrected AECL tables and the results obtained by using the method introduced in this work.

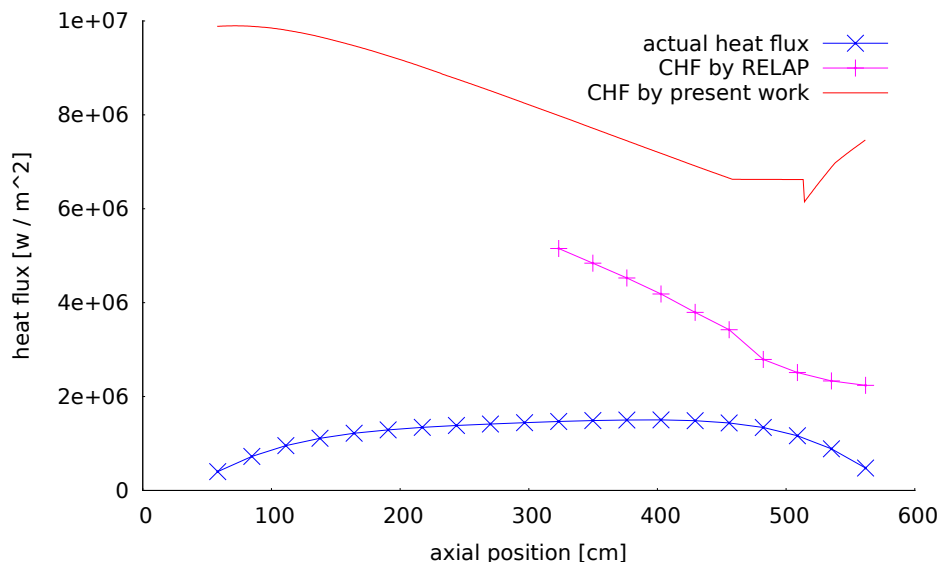


Figure 11: Actual heat flux from the fuel to the coolant and CHF limits as predicted by the computer code RELAP and by the present method for a one-dimensional coupled thermalhydraulic-neutronic model of a light-water nuclear reactor at 70 bars.

4 DISCUSSION

For light water, the sonic limit given by equation (4) switches to the one given by equation (5) approximately at twenty bars as depicted in figure 8. The wall temperature at which departure of nucleate boiling is expected to occur according to the new theory and the one-dimensional momentum conservation prediction is continuous at the switching point, and still increases with the bulk pressure but at a lower rate. The value for T_{DNB} as predicted by the explicit approximation given by equation (6) is poor and should be avoided when possible. It tends to overestimate the temperature of DNB, especially for $p_b > 5$ bar.

The function q''_{crit} illustrated in figures 9a–9d seems to give the expected behavior with respect to each of the parameters, namely the pressure, the local quality, the mass flux and the hydraulic diameter. However, there are at least two aspects that can be improved in the proposed function. First, for low negative qualities there is a discontinuity in the slope because the fit of the correction factor $F(\chi_{tt}^{-1})$ given by equation (8) has a discontinuous derivative at $\chi_{tt}^{-1} = 0.1$. A smooth expression for $F(\chi_{tt}^{-1})$ may provide better results. Additionally, the critical heat flux has a discontinuity for $x = 0$. Moreover, the proposed q''_{crit} increases sharply with the quality. This behavior does not seem to be correct. Apparently, the heat flux transfer given by the Chen correlation for positive qualities increases with x whilst the temperature of DNB does not. When the bulk fluid reaches saturation conditions, the validity of the one-dimensional momentum conservation proposed by Schroeder-Richter and Bartsch that leads to the sonic limits (4) and (5) is questionable, as stated in the original paper. A new model for the computation of extrema on the heat transfer rate for positive qualities is needed to improve the critical heat flux prediction for $x > 0$.

Figure 11 shows that the proposed function q''_{crit} apparently overestimates the critical heat flux by an appreciable amount. However, on the one hand, the order of magnitude of the estimation is correct. And on the other hand, RELAP takes into consideration the development of the flow and the influence of local geometric disturbances through a number of experimental correlations, while the proposed function does not. To take these particularities into consideration, more parameters have to be included in the function.

5 CONCLUSIONS

A prediction of the wall temperature at which departure of nucleate boiling occurs based on a new thermodynamic and mechanic non-equilibrium subcooled boiling theory was introduced by Schroeder-Richter and Bartsch (1994). This prediction uses no empirical coefficient at all. It relies only on the fluid properties at the saturation pressure. To estimate the heat flux at which departure of nucleate boiling occurs, in this paper the use of Chen's correlation is proposed. As a result, for a fixed fluid, a function of four parameters—the bulk pressure, the local quality, the mass flux and the hydraulic diameter—was constructed. It is important to remark that the function does contain only experimental coefficients—introduced by the Chen correlation—but not specific to any particular fluid. The proposed function should be applicable to any substance, provided the appropriate properties are used.

The obtained continuous function gives the expected general behavior with respect to the four parameters and the order of magnitude is correct when compared with experimental results for light water. However, the proposed function tends to overestimate the critical heat flux. Therefore, some minor corrections should be introduced in order to have a method that can be used in engineering applications. Future works will address these pending issues.

A IMPLEMENTATION

The evaluation of the critical heat flux as proposed by equation (7) needs the evaluation of algebraic expressions, both explicit and implicit and one and two-dimensional properties interpolation. Moreover, it would be convenient to exchange information with other calculation codes for example to obtain the information needed to compute the CHF estimation. Indeed, these—and a few other things—are the features that the common framework *wasora* provides to engineering calculation codes. The following file can be included from any input input belonging to the *wasora* suite, providing the four-dimensional function `chf` that can be used in the appropriate environment.

```

DEFAULT_INTERPOLATION akima

# saturated fluid properties
#####

# saturation pressure as a function of temperature
FUNCTION p_s(T) FILE h2osat.dat COLUMNS 1 2
# saturation temperature as a function of pressure
FUNCTION T_s(p) FILE h2osat.dat COLUMNS 2 1

# specific volumes, internal energies and enthalpies
FUNCTION v_f(p) FILE h2osat.dat COLUMNS 2 4
FUNCTION v_g(p) FILE h2osat.dat COLUMNS 2 16
FUNCTION u_f(p) FILE h2osat.dat COLUMNS 2 5
FUNCTION u_g(p) FILE h2osat.dat COLUMNS 2 17

FUNCTION h_f(p) = u_f(p) + p*v_f(p)
FUNCTION h_g(p) = u_g(p) + p*v_g(p)

# evaporation enthalpy
FUNCTION h_fg(p) = h_g(p) - h_f(p)

# liquid properties
FUNCTION rho_f(p) FILE h2osat.dat COLUMNS 2 3
FUNCTION mu_f(p) FILE h2osat.dat COLUMNS 2 12
FUNCTION cp_f(p) FILE h2osat.dat COLUMNS 2 9
FUNCTION k_f(p) FILE h2osat.dat COLUMNS 2 13
FUNCTION sigma_f(p) FILE h2osat.dat COLUMNS 2 14
FUNCTION a_f(p) FILE h2osat.dat COLUMNS 2 10

# vapor properties
FUNCTION rho_g(p) FILE h2osat.dat COLUMNS 2 15
FUNCTION mu_g(p) FILE h2osat.dat COLUMNS 2 24
FUNCTION a_g(p) FILE h2osat.dat COLUMNS 2 22

# compressed fluid properties
#####
FUNCTION v(p,T) FILE h2ocomp.dat COLUMNS 1 2 4
FUNCTION u(p,T) FILE h2ocomp.dat COLUMNS 1 2 5
FUNCTION h(p,T) = u(p,T) + p*v(p,T)

# gravity
g = 9.8 # [ m / s^2 ]

```

```

# parameters for computing T_DNB_approx
#####
R = 8.314          # [ j / ( mol K ) ]  gas constant
M = 18e-3         # [ kg / mol ]      molar mass
kappa_g = 1+1/3   # non-dimensional

# bulk temperature
FUNCTION T_b(p,x) = if(less(x, 0), root((h(p, T) - h_f(p))/h_fg(p) - ←
x, T, 100, 800), T_s(p))

# DNB temperature
# approximation
FUNCTION T_DNB_approx(p) = T_s(p)/(1 - R/M*T_s(p)/h_fg(p) * log(2* ←
kappa_g + 1))

# if 2*a_g(p) < a_f(p_s(T_dnb)) (eq. 4)
FUNCTION T_DNB_limit1(p) = root((v_g(p)-v_f(p_s(T)))*(p_s(T)-p)-2* ←
a_g(p)^2, T, 200, 800)
# if 2*a_g(p) > a_f(p_s(T_dnb)) (eq. 5)
FUNCTION T_DNB_limit2(p) = root((v_g(p)-v_f(p_s(T)))*(p_s(T)-p)-0.5* ←
a_f(p_s(T))^2, T, 200, 800)

FUNCTION cond1(T) = (v_g(p)-v_f(p_s(T)))*(p_s(T)-p)-2*a_g(p)^2
FUNCTION cond2(T) = (v_g(p)-v_f(p_s(T)))*(p_s(T)-p)-0.5*a_f(p_s(T)) ←
^2
FUNCTION T_DNB(p) = root(if(less(2*a_g(p), a_f(p_s(T))), cond1(T), ←
cond2(T)), T, 200, 800)

# Reynolds number
FUNCTION Re(p,G,D,H) = G*D.H/mu_f(p)

# Prandtl number
FUNCTION Pr(p) = cp_f(p)*mu_f(p)/k_f(p)

# Inverse Martinelli parameter
FUNCTION xtt(p,x) = if(greater(x,0), (x/(1-x))^0.9 * (rho_f(p)/rho_g ←
(p))^0.5 * (mu_g(p)/mu_f(p))^0.1, 0)

# Chen's correction factor
FUNCTION F(dummy_xtt) = if(less(dummy_xtt, 0.1), 1, 2.35*(dummy_xtt ←
+0.213)^0.736)

# void fraction
FUNCTION alpha(p,x) = if(greater(x,0), x/rho_g(p) / ((1-x)/rho_f(p) ←
+ x/rho_g(p)), 0)

# Modified Reynolds number
FUNCTION Re_TP(dummy_Re,p,x,dummy_xtt) = dummy_Re * (1-alpha(p,x)) * ←
F(dummy_xtt)^1.25

# Chen's suppression factor
FUNCTION S(dummy_ReTP) = if(less(dummy_ReTP, 325000), 1/(1+3.305e-6* ←
dummy_ReTP^1.14), if(less(dummy_ReTP, 700000), 1/(1+3.186e-4* ←

```

```

dummy_ReTP^0.78), 0.0797))

# convective heat transfer coefficient
FUNCTION alpha_c(p,x,G,D.H) = 0.023 * Re(p,G,D.H)^(4/5) * Pr(p) ←
    ^ (2/5) * F(xtt(p,x)) * k_f(p)/D.H

# boiling heat transfer coefficient
FUNCTION alpha_b(p,x,G,D.H) = 0.00068935*((k_f(p)^0.79 * cp_f(p) ←
    ^0.45 * rho_f(p)^0.49 * g^0.25) / (sigma_f(p)^0.5 * mu_f(p)^0.29 ←
    * h_fg(p)^0.24 * rho_g(p)^0.24)) * (T_DNB(p) - T_s(p))^0.24 * ( ←
    p_s(T_DNB(p)) - p)^0.75 * S(Re_TP(Re(p,G,D.H),p,x,xtt(p,x)))

# critical heat flux
FUNCTION chf(p,x,G,D.H) = alpha_c(p,x,G,D.H)*(T_DNB(p) - T_b(p,x)) + ←
    alpha_b(p,x,G,D.H)*(T_DNB(p) - T_s(p))

```

REFERENCES

- Chen J. Correlation for boiling heat transfer to saturated fluids in convective flow. Technical Report 64-HT-34, ASME, 1963.
- Clausse A. La crisis de ebullición: a 75 años de la curva de Nukiyama. In *Conference at Academia Nacional de Ciencias de Buenos Aires*. 2009.
- Clausse A. and Lahey R.T. The influence of flow development on subcooled boiling. *International Communications in Heat and Mass Transfer*, 17, 1990.
- Dwyer O.E. and Hsu C.J. Liquid microlayer thickness in nucleate boiling on a heated surface letters. *Heat and Mass Transfer*, 2:179–187, 1975.
- Freis D., Theler G., Mazzantini O., and Tiestch W. Investigation on thermal hydraulic effects of sub-cooled nucleate boiling. In *2011 Jahrestagung Kerntechnik*. Berlin, 2011.
- Groeneveld D.C., Leung L.K.H., Kirillov P.L., Bobkov V.P., Smogalev I.P., Vinogradov V.N., Huang X.C., and Royer E. The 1995 look-up table for critical heat flux in tubes. *Nuclear Engineering and Design*, 163:1–23, 1996.
- Mazzantini O., Schivo M., Di Cesare J., Garbero R., Rivero M., and Theler G. A coupled calculation suite for Atucha II operational transients analysis. *Science and Technology of Nuclear Installations*, Nuclear Activities in Argentina, 2011. doi:10.1155/2011/785304.
- Mitrovic J. Wärmetransport in der umgebung einer wachsenden dampfblase. *Wärme und Stoffübertragung*, 19:47–52, 1985.
- Moore F.D. and Mesler R.B. The measurement of rapid surface temperature fluctuations during nucleate boiling of water. *AIChE Journal*, 7:620–624, 1961.
- Nukiyama S. Maximum and minimum values of heat transmitted from metal to boiling water under atmospheric pressure. *International Journal of Heat and Mass Transfer*, 9:1419–1433, 1966. Originally in J. Soc. Mech. Eng. Jpn. 37 367–374 (1934).
- Schroeder-Richter D. *Ein analytischer Beitrag zur Anwendung der Thermodynamik irreversibler Prozesse auf Siedephänomene*. Ph.D. thesis, TU Berlin, 1991.
- Schroeder-Richter D. and Bartsch G. Analytical calculation of DNB-superheating by a postulated thermo-mechanical effect of nucleate boiling. *International Journal of Multiphase Flow*, 20(6):1143–1167, 1994.
- Theler G. *Non-linear analysis of the coupled thermalhydraulic-neutronic problem*. Master's Thesis, Instituto Balseiro, Argentina, 2008.
- Theler G. Milonga: a free nuclear reactor core analysis code. 2011a.

<http://ib.cnea.gov.ar/~thelerg/wasora/milonga>.

Theler G. Wanna-be Advanced Suite for Optimization and Reactor Analysis. 2011b.

<http://ib.cnea.gov.ar/~thelerg/wasora>.

Walker J. Drops of water dance on a hot skillet and the experimenter walks on hot coals.

Scientific American, 237:126, 1977.